IEEE Robotics and Automation Letters (RAL) paper presented at the
2020 IEEE/RSJ International Conference on Intelligent Robots and Systems (IROS)
October 25-29, 2020, Las Vegas, NV, USA (Virtual)

Self-Sensing and Feedback Control for a Twin Coil Spring-Based Flexible Ultrasonic Motor

Yunosuke Sato[1], Ayato Kanada[2], and Tomoaki Mashimo[1]

***Abstract*— We propose a twin coil spring-based soft actuator that can move forward and backward with extensibility and can bend left and right with flexibility. It is driven by two flexible ultrasonic motors, each consisting of a compact metallic stator and an elastic elongated coil spring. The position of the end effector is determined by the positional relationship of the two coils and can be kinetically controlled with a constant curvature model. In our design, the coil springs act not only as a flexible slider but also as a resistive positional sensor. Changes in the resistance between the stator and the coil spring end are converted to a voltage and used for position detection. Each flexible ultrasonic motor with the self-sensing is experimentally evaluated, and it has shown good response characteristics, high sensor linearity, and robustness, without losing flexibility and controllability. We build a twin coil spring-based flexible ultrasonic motor prototype and demonstrate feedback control of planar motion based on the constant curvature model.**

I. INTRODUCTION

Improving the flexibility and compliance of actuators is essential for extending the use of continuum robots in applications such as medicine and rescue [1]–[3]. One typical driving method for continuum robots uses electromagnetic motors placed at external sites to control end effectors by mechanisms such as wires (tendons) that transmit traction forces [4], [5]. In such robots, commercial rigid sensors are mostly attached to the positions of the actuators. These systems are regarded as having low controllability because their complicity increases with the number of joints between the sensors and the end effectors. The sensors can be placed directly at the joints of the end effectors; however, conventional sensors lack the softness and enlarge the joints.

With the rapid increase in the study of soft actuators, new internal sensors with softness are required, and they are designed according to the driving principles of soft actuators. The largest class of prospective soft actuators is fluidic elastomer actuators (FEA), in which soft materials (e.g., gels and elastomers) enclose fluids such as air and functional fluids [6]–[8]. They are deformed by the expansion and compression of the fluid when a voltage or air pressure is applied. For the control of FEAs, many intrinsic sensing methodologies have been proposed using a variety of principles, such as strain gauges using liquid metals (e.g., eutectic gallium-indium (eGaIn) [9], [10]), conductive rubbers [11], capacitive strain sensors [12], [13], optical fiber sensors [14], [15], hall effect sensors [16], [17], and inductive sensors [18]–[20]. These sensors have compliance and extensibility but lower resolution and linearity. Another class of soft actuators involves deformable materials that can produce a strain, such as dielectric elastomer [21], [22]. Such materials can function as self-sensing to detect their deformation [23], [24], but they have similar difficulties to other types of sensors.

We have studied a "flexible ultrasonic motor," a new kind of soft actuator designed for the use in soft continuum robots [25]. It consists of a single cubic stator with a center hole threaded with an elastic elongated coil spring. When voltages are applied to piezoelectric elements on the stator, the coil spring moves linearly. One advantage of using a coil spring is that its flexibility and stroke (the traveling distance) are designable by selecting the dimensions of the coil, such as its diameter, cross-section, and the number of turns. In this design, the coil spring has another significant advantage in terms of improving motor performance. The coil is designed to have a slightly larger diameter than the stator hole through which it passes. The force acting on the inner surface of the stator produces an optimal pre-pressure at the stator-spring interface to enhance the motor's thrust force. In our previous experiments, the actuation of a single flexible ultrasonic motor was demonstrated and evaluated. The motor succeeded in actuating a coil spring that was being sharply bent under curved constraint conditions [26]. This result have shown potential as a new soft actuator. However, none of the control strategies have yet been studied, and sensors have not yet been used to achieve control.

In this paper, we propose a coil spring-based soft actuator using two flexible ultrasonic motors, the coil ends of which are connected by a plastic component, as shown in Fig. 1. (See the accompanying video.) This actuator has been named "Twin coil spring-based flexible ultrasonic motor (Twin-coil USM)" to distinguish it from a single flexible ultrasonic motor. In addition to the two noted roles of the coil spring, its flexibility and pre-pressure, we also used it as a linear variable-resistance sensor. For this linear sensor, a thin wire is attached to either end of the coil spring. When a voltage is applied, a voltage drop occurs between one end of the coil and the stator's ground, and the position can be estimated. There are three advantages to this sensing. The first one is that no additional sensing component is required. It means that the motor can achieve control without reducing output power, flexibility, and range of motion. Secondly, this principle has linearity and results in a low calculation cost in

[1]Yunosuke Sato and Tomoaki Mashimo are with the Department of Mechanical Engineering at Toyohashi University of Technology, 1-1 Hibarigaoka, Tempaku-cho, Toyohashi, Aichi, 441-8580, Japan. y-sato@is.me.tut.ac.jp, mashimo@me.tut.ac.jp

[2]Ayato Kanada is with the Department of Mechanical Engineering at Kyushu University, 744 Motooka, Nishi-ku, Fukuoka, 819-0395, Japan. kanada@mech.kyushu-u.ac.jp

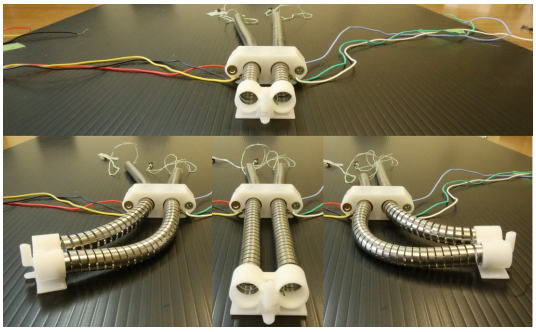

Fig. 1. Twin coil spring-based flexible ultrasonic motor (Twin-coil USM).

comparison with non-linear soft sensors. The third advantage is that the sensor output determined by the distance between the stator and the end of the coil is very stable, even when an external force acts on the coil and increases its deformation.

The rest of this paper is organized as follows. Section II explains the principles of the flexible ultrasonic motor and the coil spring-based position sensor. A prototype sensor system embedded in a flexible ultrasonic motor is built, and the performance parameters, such as a sensing accuracy and frequency response, are examined in Section III. Finally, Section IV demonstrates the Twin-coil USM with a feedback control system.

II. DESIGN AND FABRICATION

A. Overview of Drive Principle and Design

We introduce the driving principle of the single flexible ultrasonic motor briefly [26]. Fig. 2(a) shows a schematic of the stator. Four piezoelectric elements adhere to the four sides of the metallic cube. The metallic part of the stator is a phosphor bronze cube of edge length 14 mm with a center hole of 10 mm in diameter. The inside of the hole is coated by electroless nickel plating with a thickness of 10 μm to prevent damage and wear being caused by contact with the coil spring. Each piezoelectric plate has a length of 14 mm, a width of 10 mm, and a thickness of 0.5 mm, and has two silver electrodes on one side for applying two different voltages. As shown in Fig. 2(b), two vibration modes are used as the driving principle to move the coil spring slider linearly. Mode 1 is a vibration that repeats expansion and contraction symmetrically about the center cross-section, and Mode 2 is asymmetrical. When both vibration modes are excited simultaneously at the same resonance frequency, the stator produces an elliptical orbit (lower right in Fig. 2(b)). This elliptical orbit moves the coil linearly by friction between the stator and the coil. When two voltages are applied to the piezoelectric elements (Fig. 2(c)), both modes are excited at the same driving frequency. These voltages are expressed as

$$E_1 = A_E \sin(2\pi f_E t) \tag{1}$$

$$E_2 = A_E \sin(2\pi f_E t + \phi) \tag{2}$$

where A_E and f_E are the amplitude and frequency of the voltages, respectively, and ϕ is the phase between the two

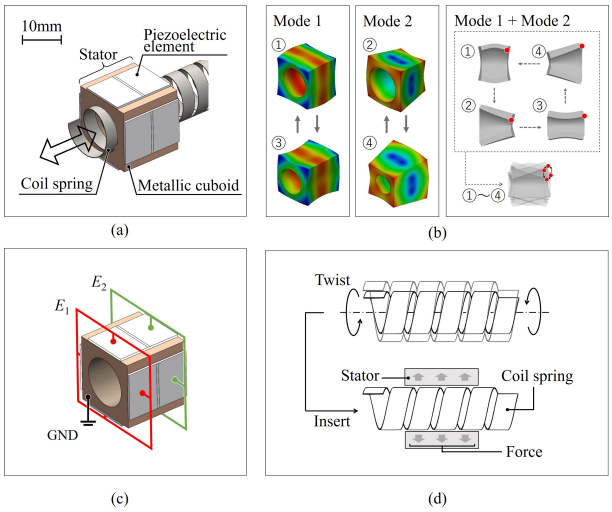

Fig. 2. Driving principle of the flexible ultrasonic motors. (a) Schematic of the motor. (b) Two vibration modes (Mode 1 and Mode 2) generated by stator and an elliptical motion. (c) Applied voltages for the motor. (d) Pre-pressure mechanism by using coil spring slider.

voltages. The frequency f_E can be tuned to the resonance frequency of the two vibration modes. The coil moves forward when the phase ϕ is set to $\pi/2$, and backward when ϕ is $-\pi/2$.

In general, ultrasonic motors that use friction as their driving principle require a pre-pressure between the stator and the slider/rotor to enhance the force/torque. They need an additional mechanism and components to generate and optimize the pre-pressure. In our design, the coil spring works not only as the coil slider but also as the pre-pressure mechanism. As shown in Fig. 2(d), the diameter of the coil is slightly larger than that of the stator hole. When the coil is twisted appropriately in the circumferential direction, its diameter decreases, and it can be smoothly inserted into the stator hole. When the torsional force is removed, the coil expands in the radial direction, generating a pre-pressure without the need for additional components.

B. Self-Sensing Using the Coil Spring

We present a new sensing methodology to detect the displacement of the coil spring slider. As mentioned above, the coil spring inserted into the stator hole has two essential roles: flexibility and pre-pressure. In this study, we also uses the coil as a linear resistive sensor. In other words, this single flexible ultrasonic motor behaves like a linear resistive potentiometer, which is a kind of three-terminal resistor consisting of an electrical resistance and a sliding contact. Fig. 3(a) shows the self-sensing design concept for the coil. The coil and the stator are treated as the resistance element and the sliding contact of a linear potentiometer, respectively. When a voltage is applied to the ends of the coil, a voltage drop occurs between each end and the stator, which is at ground potential. When the coil moves, the voltage drop changes continuously in proportion to the displacement of the coil, and its position can be measured. One advantage

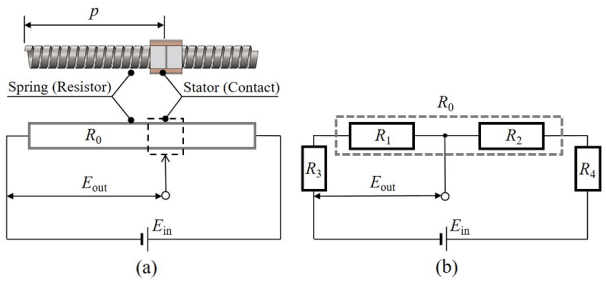

Fig. 3. Principle of self-sensing using the coil. (a) Mechanical components and the simplified electrical model. (b) Detailed electrical model.

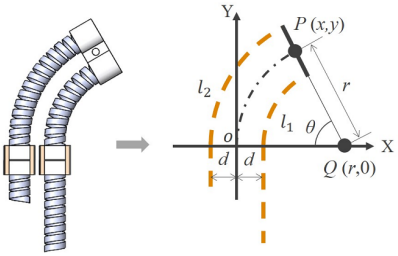

Fig. 4. Constant curvature model for the twin coil spring-based flexible ultrasonic motor.

of using such a potentiometer is the stability inherent in the electrical connection between the resistance element and the stator. In the design of the coil, the coil expands in the radial direction and makes firm contact with the inner surface of the stator hole. Wherever the stator is located along the resistance element, the electrical connection remains stable.

Fig. 3(b) shows an electrical model of the potentiometer. We define the resistance of the whole coil as R_0, and the stator divides it into R_1 and R_2. The resistances of the wires are denoted as R_3 and R_4. When a voltage E_{in} is applied to both ends of the coil, the output voltage E_{out} is obtained as

$$E_{\text{out}} = \frac{R_3 + R_1}{R_1 + R_2 + R_3 + R_4} E_{\text{in}}. \tag{3}$$

This is the output voltage from the potentiometer. With the cross-sectional area S and electrical resistivity ρ of the coil spring, the relative position of the coil spring to the stator is expressed as

$$p = \frac{S}{\rho} R_1. \tag{4}$$

When (4) is substituted into (3), the position p is obtained from the measured voltage E_{out}.

$$p = \frac{S}{\rho} \left(\frac{R_0 + R_3 + R_4}{E_{\text{in}}} E_{\text{out}} - R_3 \right). \tag{5}$$

Since all variables in (5) are constant, it can be rewritten using the arbitrary constants C and D, as follows:

$$p = C E_{\text{out}} + D. \tag{6}$$

This equation shows that the relationship between the measured voltage E_{out} and the position p is linear.

C. Constant Curvature Model

We model the motion of the Twin-coil USM to estimate the position of the end effector. The constant curvature model is a well-known forward kinematics formula for continuum robots [27]. A Twin-coil USM with two flexible ultrasonic motors can move and bend the end effector by the relationship between the two coils. Considering that the coils will move on a plane in the experiments, as described in a later section, we use a planar constant curvature model to express the motion.

Fig. 4 shows a schematic of the constant curvature model. The position of the end effector is expressed as $P_x = r(1 - \cos\theta)$ and $P_y = r\sin\theta$. Here, r is the bend radius and θ is the angle between the x-axis and the line PQ. The solid lines represent the coil springs of the Twin-coil USM. The springs are held at a distance of $2d$ from each other. The arc lengths of the coil springs (i.e., the dashed lines in the range $y > 0$) are set to l_1 and l_2. Using the arc lengths l_1 and l_2 and the distance d, the end effector's position $P_x = r(1 - \cos\theta)$ and $P_y = r\sin\theta$ can be expressed as follows:

$$P_x = \frac{(l_1 + l_2)d}{l_2 - l_1} \left(1 - \cos \frac{l_2 - l_1}{2d} \right). \tag{7}$$

$$P_y = \frac{(l_1 + l_2)d}{l_2 - l_1} \sin \frac{l_2 - l_1}{2d}. \tag{8}$$

These equations are the forward kinematics equation $f(l_1, l_2) = (P_x, P_y)$. The solution of the inverse kinematics equation $f^{-1}(P_x, P_y) = (l_1, l_2)$ can be solved numerically. Note that this constant curvature model ignores the influence of disturbances, such as external forces.

III. EXPERIMENTS

A. Evaluation of Self-Sensing

The self-sensing apparatus is built and experimentally evaluated. During the experiments, a constant voltage E_{in} of 140 mV is applied to the coil spring. The output voltage E_{out} is amplified to 55 times by an amplifier circuit because the original signal is very low. This value is converted by a 10-bit analog-to-digital (AD) converter with a reference voltage of 5 V. The voltages obtained are averaged over 10 measurements to reduce noise. Fig. 5(a) shows the behavior of the sensor output when the coil moves. In the abscissa axis, the displacement between one end of the coil spring and the front surface of the stator is taken from 0 mm to 100 mm in 10 mm steps. In this experiment, the coil spring is manually moved using a scale. The error bars indicate the standard deviation from five tests at each position. The results show that the relationship between the displacement and the output voltage is linear, and the maximum standard deviation is 28.1 mV. The constants in (6) are obtained by approximating this result by a least-squares method (C = 26.6 and D = 34.5).

We examine how the sensor output changes when applying external forces such as those experienced when bending,

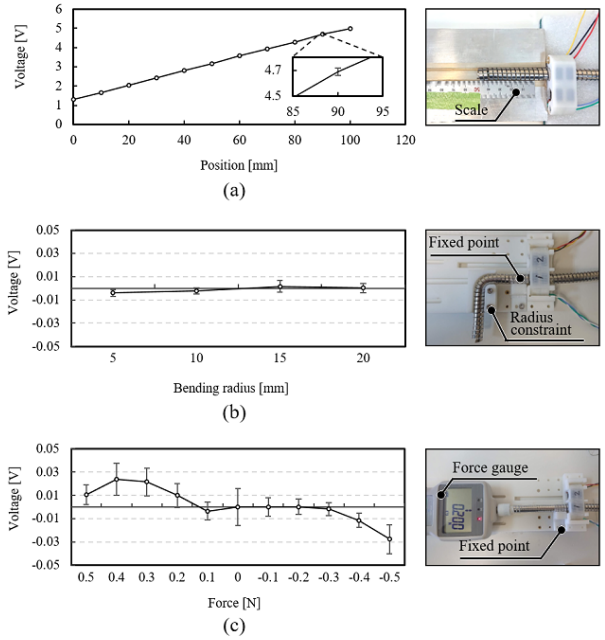

Fig. 5. Change in the sensor output when (a) the coil moves linearly, (b) the coil bends, and (c) the coil extends and contracts. (Error bars indicate SD from five tests of one condition).

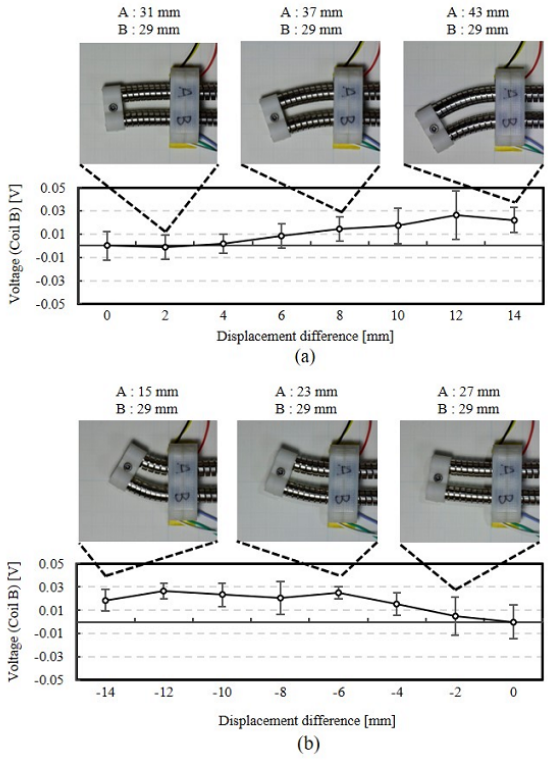

Fig. 6. Change in the sensor output from coil B when the displacement when the displacement of coil A increases (a) and decreases (b). The displacement difference (abscissa) is the subtraction of coil A from coil B. (Error bars indicate SD from five tests of one condition).

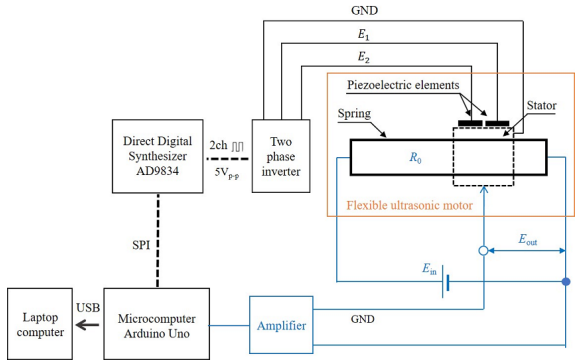

Fig. 7. Feedback control circuit for the flexible ultrasonic motor with self-sensing.

extending, or contracting the coil spring. In the experiments, the output voltages in each condition are measured five times. The coil spring is set to a displacement of 50 mm and is fixed by insulating tape. The coil springs are set in constraint components with a radius of 5, 10, 15, or 20 mm. Fig. 5(b) shows the voltage change for each bending radius. The voltage change is slight at all bending radii, and the maximum is less than 4.0 mV even at a bending radius of 5 mm. This value is as small as the resolution of the AD converter.

The sensor output with the expansion and contraction of the coil is evaluated. One end of the coil spring is fixed to a force gauge to measure the restoring force. The voltage is measured while the restoring force changes from -0.5 N to $+0.5$ N in 0.1 N steps (negative values indicate compression). Fig. 5(c) shows the variation in voltage with changing force. When the restoring force is 0 N in the coil, the output voltage is defined as 0 V. The variation in the output voltage occurs by the change in the contact condition between the stator (electrical contact) and the coil spring (resistance). As the coil spring compresses, the gap of the coils reduces. At $-$ 0.5 N, the coils contact and lower the electric resistance. The output voltage is approximately $-$ 27.5 mV, which is equivalent to a displacement of 0.73 mm in this displacement sensor. Because it is smaller than the maximum standard deviation of the linear movement (Fig. 5(a)), the resulting sensor has sufficient robustness against disturbance.

Another important aspect is the implementation of the sensing methodology into the Twin-coil USM. Let us examine how the output signal of the sensor varies when the two coils form a curve in the Twin-coil USM. Fig. 6 shows the sensor output from coil B when coil A moves and coil B is stationary. The output voltage slightly increases at a larger displacement of coil A (Fig. 6(a)), and vice versa (Fig. 6(b)). The voltage change is 26.6 mV (a displacement of 0.71 mm) at maximum.

B. Feedback Control Experiment

We build a feedback control system consisting of a single flexible ultrasonic motor and the self-sensing. Fig. 7 shows the self-sensing feedback control loop. This circuit includes

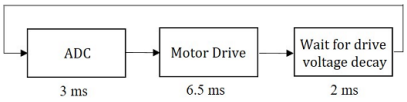

Fig. 8. Time table of the control cycle.

a central processing unit (an Arduino Uno), a two-phase inverter, a direct digital synthesizer (DDS), an amplifier, and a PC. To drive the flexible ultrasonic motor, the two-phase inverter converts a rectangular wave of 5 V_{p-p} from the DDS into a sine wave of 120 V_{p-p} by a bridge circuit and an LC filter circuit. To control the position and speed of the flexible ultrasonic motor, the Arduino changes the frequency and phase of the rectangular wave by communication through the Serial Peripheral Interface (SPI). A USB cable connects the PC and Arduino.

One of the technical problems in the control system is that the actuation voltage and the sensing signal use the same terminal of the stator, as shown in Fig. 2 and Fig. 3. The sensor, therefore, suffers from noise due to the high driving voltage applied while the motor is moving. To overcome this problem, we implemented a program to divide the operating time into two separate sensing and actuation periods in one control cycle of 11.5 ms, as shown in Fig. 8. In the initial period of 3 ms, the AD converter reads the output voltage from the sensor. For the next period of 6.5 ms, the driving voltage is applied to the flexible ultrasonic motor. The remaining 2 ms is a waiting time for the safety of the system. The proportion of actuation time in one cycle is about 60%, and this reduces the speed of the motor. These times were determined experimentally to obtain stable movement.

Next, we consider how to control the motion of the flexible ultrasonic motor. The flexible ultrasonic motor changes its velocity and traveling direction by modulating the frequency f_E and the phase ϕ of the applied voltages, respectively, as described by (1) and (2). Fig. 9 shows the forward velocity ($\phi = \pi/2$) and the backward velocity ($\phi = -\pi/2$) of the motor when the frequency of the applied voltages is changed from 81.0 kHz to 84.5 kHz. The error bars show the standard deviations of five experiments because the coil vibrates in the traveling direction during the motion. Although there is a difference between the forward and backward velocities, both velocities peak at the resonance frequency (81.5 kHz) and gradually decrease at higher frequencies. Using these characteristics, it is possible to control the motion of the flexible ultrasonic motor by adjusting the driving frequency f_E between 81.5 kHz and 84.5 kHz. The difference between the forward and backward velocities is due to experimental factors such as fabrication and adhesion of the piezoelectric elements.

Fig. 10 shows the closed-loop position control scheme. The proportional (P) controller determines the frequency f_E and the phase difference ϕ based on the displacement error e. Since the motor velocity depends on the traveling direction, the constant of P controller has different values in the forward and backward directions. Although the relationship between

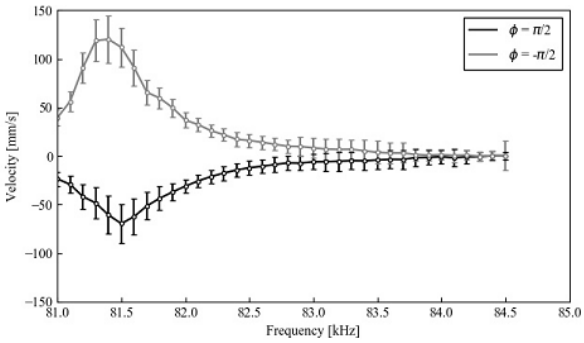

Fig. 9. Relationship between the velocity and the driving frequency. (Errorbars indicate SD from five tests of one frequency).

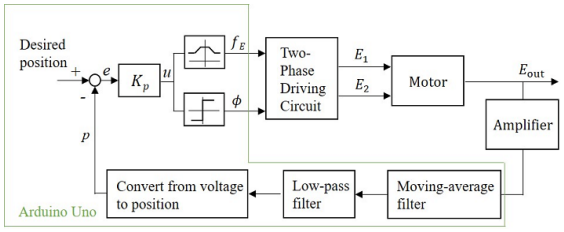

Fig. 10. Feedback control scheme.

the voltage frequency and the velocity is non-linear, we assume it as linear for simplicity. The displacement of the coil is estimated by measuring the amplified voltage $E_{\rm out}$. To reduce noise, the output signal passes through a 10-sample moving-average filter and a low pass filter with a cutoff frequency of 100 Hz.

We investigate the frequency response of the feedback control system. Fig. 11 shows the bode plot when reference sine waves of between 0.1 and 5 Hz and a constant amplitude of 60 mm are given as an input. The controller is able to follow the inputs up to about 0.5 Hz without any delay. Although the response depends on the reference displacement, the results show a good response characteristic in comparison with other linear motors because the inertia of the coil spring is very low for a generated torque.

IV. DEMONSTRATION OF A TWIN-COIL USM

We build a Twin-coil USM using two flexible ultrasonic motors and demonstrate its feedback control. Fig. 12(a) shows a schematic diagram of the Twin-coil USM, in which the two coils are aligned in parallel, and the ends of the coils are connected to form an end effector. The two stators are fixed to a housing part, and the distance between their centers is approximately 17 mm. As shown in Fig. 12(b), flexible bronze electrodes are attached to the housing to stabilize the electrical contact with the piezoelectric elements on the stator. Although the end effector fixes one end of each coil, the other end remains free. The end effector of the Twin-coil USM can move and bend by controlling the displacement of the two coils. To control the two coils, we added a two-phase inverter and a DDS to the control circuit shown in Fig. 7.

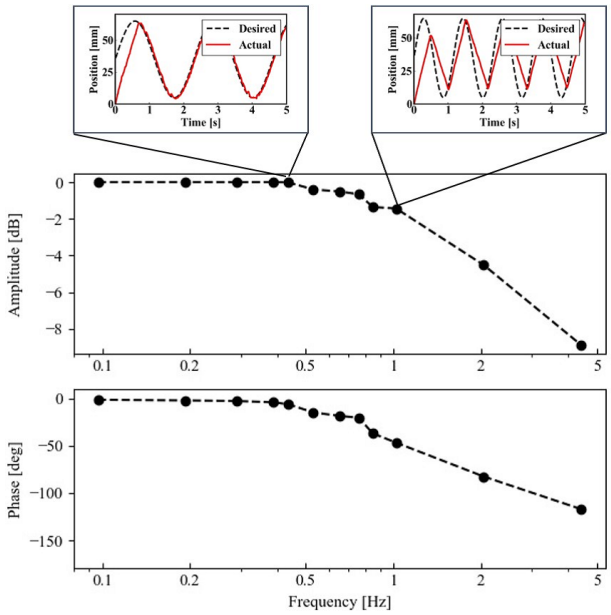

Fig. 11. Bode plot for the flexible ultrasonic motor.

For the demonstration of feedback control, a circle with a diameter of 25 mm at a position 35 mm away from the edge of the stator's housing is set as the desired trajectory. This circle is approximated by a 36-sided polygon prepared from an inverse kinematics correspondence table. The end effector is made to draw the same circle four times at a constant speed (11.5 s per lap) to evaluate repeatability. The motion of a marker on the end effector is tracked by a camera with a frame rate of 30 Hz (Fig. 12(c)). The sensor outputs from the two coils are also recorded at the same time. The experimental conditions to drive the motor and sense position are the same as the previous section.

Fig. 13 shows the response of each coil spring as measured by the self-sensing. The position of each coil spring shows a good agreement with the desired trajectory from the constant curvature model, without overshoot or delay. This result means that the end effector should have drawn the desired circle, but the actual motion showed an unexpected trajectory. Fig. 14 shows the motion of the end effector obtained by the camera. The recorded trajectory appears as a distorted ellipse, and it repeats the almost same trajectory four times. The difference between the sensor and the camera is caused by external forces and friction. It can be clearly seen in the x-direction, even though the stators move the coil based on the constant curvature model. There are two probable reasons for this: (1) friction between the end effector, and the ground restricts the motion, and (2) the stiffness of the proposed actuator in the x-direction is lower than that in the y-direction due to the inherently elongated structure of the spring. In fact, when we lift the end effector to remove the friction, the end effector moves to the desired circle in the neighborhood of positions of (b) and (d).

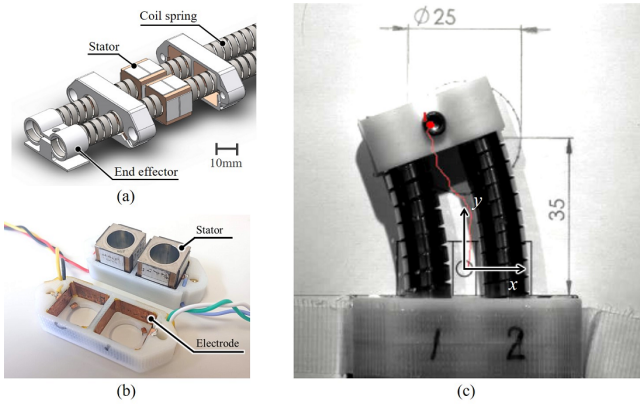

Fig. 12. Structure of Twin-coil USM. (a) Schematic diagram of Twin-coil USM. (b) Housing and electrodes for the stator. (c) Image taken by 2D tracking camera for tracking end effector.

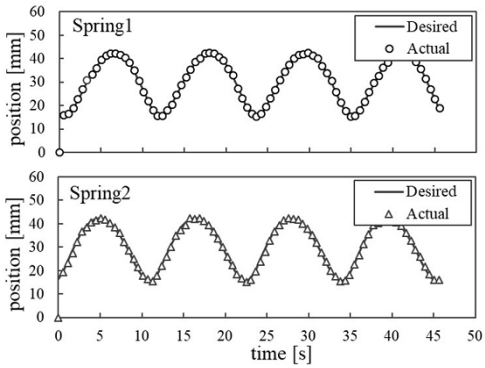

Fig. 13. The signals from the two coil spring-based resistive sensors. They are in good agreement with the curve from the constant curvature model.

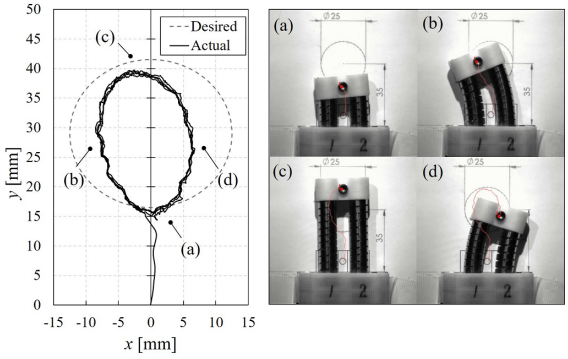

Fig. 14. Experimental circular motion obtained by the camera. Four snapshots from (a) to (d) are accorded to the points in the ellipse trajectory during the motion.

V. CONCLUSIONS

We proposed a self-sensing-based soft sensor for a flexible ultrasonic motor and demonstrated the feedback control of a Twin-coil flexible ultrasonic motor. Hence, the elastic elongated coil had three important functions: the flexibility (compliance), pre-pressure, and resistance sensor. This sensor was able to obtain a good positioning accuracy less than an error of 0.75 mm and linearity over a wide range of motion

from 0 mm to 100 mm. Furthermore, the system showed high electrical stability even when the coil spring was sharply bent with a minimum radius of 5 mm or pulled/pushed with a maximum force of 0.5 N. A feedback control system was constructed and evaluated experimentally. A single flexible ultrasonic motor with a resistive sensor showed a frequency response that was able to follow an input of up to about 0.5 Hz without degradation of gain or phase delay. We built a Twin-coil USM using two flexible ultrasonic motors and implemented a feedback control of tracking a desired trajectory, but an unexpected error between the camera and the resistive sensor occurs. In future work, we will derive a correct model based on the modified constant curvature model incorporating friction and external forces.

The proposed sensor-actuator system is still under development, and there are many ways it can be improved. First, the noise resistance, which is robustness against the influence of external noise, can be enhanced. Since the coil spring is made from stainless steel and has low resistance, the sensor requires a very low voltage to minimize power consumption and heat dissipation, which results in weak noise resistance. Increasing the electrical resistance by an electrostatic coating can increase the resolution of the sensor and its susceptibility to noise. Second, the motor response can be improved. The controller restricts the motor response by alternating the operation between sensing and actuation in a control cycle. Electrically insulating a part of the stator to separate the sensing and actuation grounds would allow the controller to drive both the sensor and the actuator simultaneously, improving the motor response. Third, it would be possible for the sensor to measure more complex motion without changing its structure or adding additional components. Although the proposed sensor only measures the displacement of the coil, it is known that the strain of a coil spring can be estimated by measuring its inductance [20]. Inductance-based self-sensing could also be embedded in our proposed system without the need for extra mechanical parts.

ACKNOWLEDGMENT

This research has been supported in part by JSPS KAKENHI Grant Number 19H02110.

REFERENCES

[1] D. Trivedi, C. D. Rahn, W. M. Kier, and I. D. Walker, "Soft robotics: Biological inspiration, state of the art, and future research," *Applied bionics and biomechanics*, vol. 5, no. 3, pp. 99–117, 2008.

[2] S. Kim, C. Laschi, and B. Trimmer, "Soft robotics: a bioinspired evolution in robotics," *Trends in biotechnology*, vol. 31, no. 5, pp. 287–294, 2013.

[3] J. Burgner-Kahrs, D. C. Rucker, and H. Choset, "Continuum robots for medical applications: A survey," *IEEE Transactions on Robotics*, vol. 31, no. 6, pp. 1261–1280, 2015.

[4] I. D. Walker, "Continuous backbone "continuum" robot manipulators," *Isrn robotics*, vol. 2013, pp. 1–19.

[5] H.-S. Yoon and B.-J. Yi, "A 4-dof flexible continuum robot using a spring backbone," in *2009 International Conference on Mechatronics and Automation*. IEEE, 2009, pp. 1249–1254.

[6] K. Suzumori, S. Iikura, and H. Tanaka, "Applying a flexible microactuator to robotic mechanisms," *IEEE Control systems magazine*, vol. 12, no. 1, pp. 21–27, 1992.

[7] C. D. Onal, X. Chen, G. M. Whitesides, and D. Rus, "Soft mobile robots with on-board chemical pressure generation," in *Robotics Research*. Springer, 2017, pp. 525–540.

[8] R. K. Katzschmann, A. D. Marchese, and D. Rus, "Hydraulic autonomous soft robotic fish for 3d swimming," in *Experimental Robotics*. Springer, 2016, pp. 405–420.

[9] J. Morrow, H.-S. Shin, C. Phillips-Grafflin, S.-H. Jang, J. Torrey, R. Larkins, S. Dang, Y.-L. Park, and D. Berenson, "Improving soft pneumatic actuator fingers through integration of soft sensors, position and force control, and rigid fingernails," in *2016 IEEE International Conference on Robotics and Automation (ICRA)*. IEEE, 2016, pp. 5024–5031.

[10] Y. Hao, Z. Liu, Z. Xie, X. Fang, T. Wang, and L. Wen, "A variable degree-of-freedom and self-sensing soft bending actuator based on conductive liquid metal and thermoplastic polymer composites," in *2018 IEEE/RSJ International Conference on Intelligent Robots and Systems (IROS)*. IEEE, 2018, pp. 1–9.

[11] P. H. Nguyen, S. Sridar, W. Zhang, and P. Polygerinos, "Design and control of a 3-chambered fiber reinforced soft actuator with off-the-shelf stretch sensors," *International Journal of Intelligent Robotics and Applications*, vol. 1, no. 3, pp. 342–351, 2017.

[12] M. C. Yuen, H. Tonoyan, E. L. White, M. Telleria, and R. K. Kramer, "Fabric sensory sleeves for soft robot state estimation," in *2017 IEEE international conference on robotics and automation (ICRA)*. IEEE, 2017, pp. 5511–5518.

[13] M. C. Yuen, R. Kramer-Bottiglio, and J. Paik, "Strain sensor-embedded soft pneumatic actuators for extension and bending feedback," in *2018 IEEE International Conference on Soft Robotics (RoboSoft)*. IEEE, 2018, pp. 202–207.

[14] S. Sareh, Y. Noh, M. Li, T. Ranzani, H. Liu, and K. Althoefer, "Macrobend optical sensing for pose measurement in soft robot arms," *Smart Materials and Structures*, vol. 24, no. 12, p. 125024, 2015.

[15] H. Zhao, K. O ' Brien, S. Li, and R. F. Shepherd, "Optoelectronically innervated soft prosthetic hand via stretchable optical waveguides," *Science Robotics*, vol. 1, no. 1, p. eaai7529, 2016.

[16] S. Ozel, N. A. Keskin, D. Khea, and C. D. Onal, "A precise embedded curvature sensor module for soft-bodied robots," *Sensors and Actuators A: Physical*, vol. 236, pp. 349–356, 2015.

[17] M. Luo, Y. Pan, E. H. Skorina, W. Tao, F. Chen, S. Ozel, and C. D. Onal, "Slithering towards autonomy: a self-contained soft robotic snake platform with integrated curvature sensing," *Bioinspiration & biomimetics*, vol. 10, no. 5, p. 055001, 2015.

[18] W. Felt, K. Y. Chin, and C. D. Remy, "Contraction sensing with smart braid mckibben muscles," *IEEE/ASME Transactions on Mechatronics*, vol. 21, no. 3, pp. 1201–1209, 2015.

[19] W. Felt, M. J. Telleria, T. F. Allen, G. Hein, J. B. Pompa, K. Albert, and C. D. Remy, "An inductance-based sensing system for bellows-driven continuum joints in soft robots," *Autonomous robots*, vol. 43, no. 2, pp. 435–448, 2019.

[20] O. Azami, D. Morisaki, T. Miyazaki, T. Kanno, and K. Kawashima, "Development of the extension type pneumatic soft actuator with built-in displacement sensor," *Sensors and Actuators A: Physical*, vol. 300, p. 111623, 2019.

[21] A. O ' Halloran, F. O ' malley, and P. McHugh, "A review on dielectric elastomer actuators, technology, applications, and challenges," *Journal of Applied Physics*, vol. 104, no. 7, pp. 071 101 – 071 101, 2008.

[22] Y. Bar-Cohen, "Electroactive polymers as artificial muscles-reality and challenges," in *19th AIAA Applied Aerodynamics Conference*, 2001, pp. 1–9.

[23] T. A. Gisby, B. M. O'Brien, and I. A. Anderson, "Self sensing feedback for dielectric elastomer actuators," *Applied Physics Letters*, vol. 102, no. 19, p. 193703, 2013.

[24] K. Jung, K. J. Kim, and H. R. Choi, "A self-sensing dielectric elastomer actuator," *Sensors and Actuators A: Physical*, vol. 143, no. 2, pp. 343–351, 2008.

[25] A. Kanada, T. Mashimo, and K. Terashima, "Flexible ultrasonic motor using an output coil spring slider," in *2017 IEEE/RSJ International Conference on Intelligent Robots and Systems (IROS)*. IEEE, 2017, pp. 5616–5621.

[26] A. Kanada and T. Mashimo, "Design and experiments of flexible ultrasonic motor using a coil spring slider," *IEEE/ASME Transactions on Mechatronics*, 2019.

[27] R. J. Webster III and B. A. Jones, "Design and kinematic modeling of constant curvature continuum robots: A review," *The International Journal of Robotics Research*, vol. 29, no. 13, pp. 1661–1683, 2010.